International Journal of Offshore and Coastal Engineering
Vol.6 | No. 2 | pp. 59 – 66 | November 2022
DOI:10.19026/ijoce.9.1369
ISSN: 2040-7459; e-ISSN: 2040-7467

Submitted: July 7, 2022 | Revised: September 10, 2022 | Accepted: October 21, 2022

Hydrodynamic Performance Analysis of Vertical Axis Water Turbine (VAWT) Gorlov Type with Hydrofoil Thickness and Inclination Angle Variables using Computational Fluid Dynamics (CFD) Approaches

Wisnu Wardhana[a,*], Shade Rahmawati[a], Dendy Satrio[a], and Annisa A. Nurliana[a]

[a)] Department of Ocean Engineering, Institut Teknologi Sepuluh Nopember, Kampus ITS – Sukolilo, Surabaya 60111, Indonesia
*Corresponding author: wisnu@oe.its.ac.id

ABSTRACT

The issue of renewable and eco-friendly energy has become the focus of research in several countries to encourage eco-friendly alternative energy. One of them is by using turbines to produce electrical energy. Vertical Axis Water Turbine (VAWT) can be an exciting research object because it has various advantages. VAWT has a simpler structure, can move at relatively slow currents and is famous for its tendency to move regardless of the water flow directions. In this study, the experimental turbine from secondary data numerically simulates using the Computational Fluid Dynamics (CFD) method with the help of ANSYS V18.1 software. The Gorlov turbine model is manufactured in 3 dimensions under steady-state flow conditions. Validation is carried out after obtaining numerical results with the mean error rate being less than 10%. The variables in this research are the thickness of hydrofoil using NACA 0010, NACA 0016, NACA 0020, and variations in inclination angle of the blade for 25^0 and 60^0. After comparing the simulation results in the form of torque values is done, it is shown that the best turbine performance is given by water turbine using NACA 0016 with 60^0 of inclination angle.

Keywords: *gorlov turbine, hydrofoil thickness, inclination angle, CFD, torque.*

1. INTRODUCTION

The increasing use of energy derived from fossil fuels and its increasingly limited availability in nature forces them to look for alternative energy sources. In Indonesia, there are still many areas that are lacking, and even electricity facilities are unavailable. Based on the data from the Ministry of Energy and Mineral Resources (ESDM) of August 2019, the national electrification ratio reached 98.86% [1]. The verification results of PT PLN (Persero), in 2019, around 1,103,859 households must be electrified. It is also stated that based on Bappenas data in 2014, 96% of electricity demand in Indonesia is still dominated by fossil fuels, namely oil, gas, and coal [2]. Meanwhile, the use of fossil fuels causes pollution, which has a destructive impact and is also difficult to renew. Alternative renewable energy solutions are options that are deemed appropriate and can be applied to solve the problem of cheap and equally distributed electricity.

Indonesia has considerable renewable energy potential, especially as a maritime country, where the total area of the oceans reaches nearly 8 million km^2 but is still not optimally utilized. Indonesia can take advantage of the potential for energy that comes from the sea, namely ocean currents. One of them is by using turbines to produce electrical energy. Currently, the horizontal axis water turbine (HAWT) type water turbine has been widely made, used and developed, compared to the vertical axis water turbine (VAWT) type, because HAWT has a better efficiency value than VAWT in utilizing wind to become electricity. However, the VAWT type has several advantages over the HAWT type, including because of the characteristics of the VAWT, which has a simpler structure, can move at relatively slow currents, can receive current from all directions and can be combined with other architectural, structural concepts, it is also easy to install a gearbox, generator and bearing [3].

The advantages mentioned make VAWT a technology that does not require too much cost and is easy to implement, making it suitable to be developed for hydroelectric powerplant in remote and underdeveloped areas. The development of VAWT itself can also be applied as another alternative to reduce dependence on the supply of electrical energy originating from fossil resources. Research on VAWT itself actually started in the 1920s and began to be developed again in the 1970s when there was an oil embargo. One type of VAWT that is widely researched and developed is the Gorlov type which basically has a working principle which is more or less the same as the Darrieus type, utilizing lift force to rotate the rotor [4]. The foil of the Gorlov Helical Turbine (GHT) type is symmetrical and can rotate in both directions equally good enough.

Several methods can be applied to obtain water turbine efficiency values. Computational Fluid Dynamics, commonly known as CFD, simulates the fluid phenomenon and its interaction with a water turbine. The CFD method became known around the 1970s with a working principle that combined physical problems, numerical calculations and took advantage of the help of computer skills to solve fluid mathematical equations based on the laws of energy, momentum, and mass conversion. The equation that occurs in fluid flow is solved discreetly by using a regulated volume. CFD can represent conditions in the field with a computer-assisted numerical analysis approach and related software [5].

The authors conducted a VAWT analysis of the Gorlov type using the Computational Fluid Dynamic (CFD) approaches in this final project research. The CFD method was chosen because the solution involved the interaction of fluids in the entire system to produce reasonably accurate results. CFD-based software, ANSYS Fluent 16, is used to simulate variations in several design variables to determine the hydrodynamic performance of vertical axis turbines. The CFD simulation validation is done by comparing the computational results in the form of moment coefficient (Cm), power coefficient (Cp), Tip Speed Ratio (TSR) with secondary experimental data.

2. BASIC THEORY

2.1 Water Turbines

Turbines, according to KBBI, are machines or motors whose wheels are pivoting with propellers driven by fluid, in this case, water. According to Kasharjanto in Wave Volume 11: 2 Journal [6], there are two types of turbine types:

a. Horizontal Type Turbine

This type of turbine has a shaft parallel to the x-axis or can have a particular slope with the x-axis.

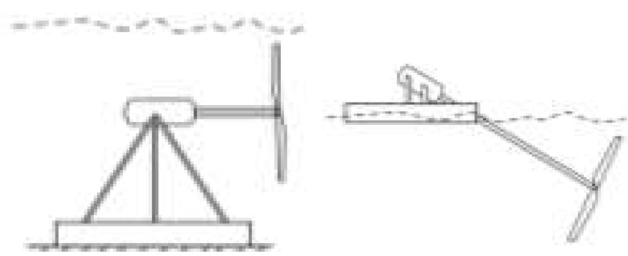

Figure 1. Horizontal Type Ocean Turbine [7]

b. Vertical Type Turbines

Unlike the horizontal turbine, this turbine has a shaft perpendicular to the x-axis or direction of ocean currents. Several types of vertical turbines have been tried, including Savionus, Darrieus, and H rotors.

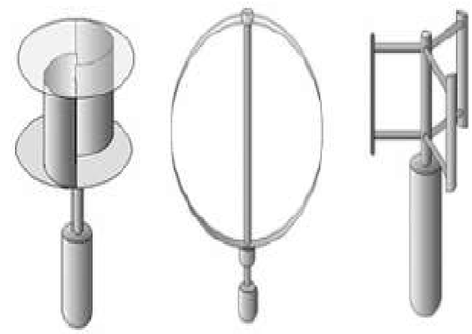

Figure 2. Vertical Type Ocean Turbine [7]

2.2 Gorlov Turbine

Gorlov turbine is a type of water turbine that Alexander M. Gorlov developed in 1995. This turbine was developed from the Darrieus turbine type, but the blade of the Gorlov turbine is helical. This turbine can be vertical or horizontal type.

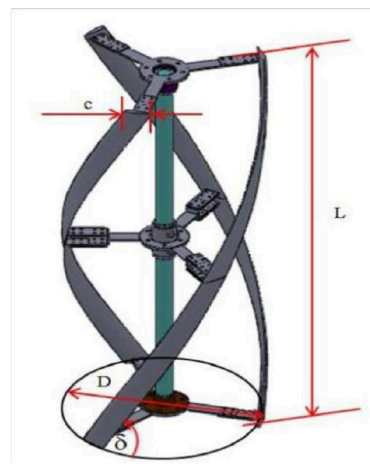

Figure 3. Gorlov Turbine [8]

Gorlov type vertical turbines have several advantages over other types, namely:

- Able to operate from all directions
- Efficiency reaches 35 percent
- Can move at low speeds (0.6 m / s) so that it can be placed anywhere.
- Simple structure

2.3 Tip Speed Ratio

The tip speed ratio is the ratio of the speed of the wind to the speed of the tip of the propeller.

$$TSR\ (\Lambda) = \frac{Blade\ Tip\ Speed}{Free\ Fluid\ Velocity} \quad (1)$$

$$TSR\ (\Lambda) = \frac{\omega R}{Vo} \quad (2)$$

turbine shaft, and Vo is free fluid velocity.

TSR is one of the most critical factors in turbine design.

If the rotor of a turbine moves slowly, many currents do not move to the helical blade. Meanwhile, if the turbine rotor moves very fast, the surrounding water will experience turbulence which will cause an imbalance in energy conversion. If the TSR value is above 1, the blade speed is faster than the wind speed. If TSR is below 1, the drag coefficient enlarges. Knowing the TSR will facilitate modeling so that the model is designed to be more efficient and maximum in generating power. The higher the TSR, the blade will be smoother [9]. Research on the development of this turbine technology is currently being carried out [10-13].

2.4 Power Coefficient

The coefficient of power is also significant to know in designing a turbine. Measurement of turbine efficiency is closely related to the power coefficient and TSR.

$$Cp = \frac{Pt}{Pa} = \frac{M\omega}{\frac{1}{2}\rho S V o^3} \tag{3}$$

Where Pt is the output power of the turbine, Pa is power available from ocean currents, M is total moment produced by the turbine, ω is turbine angular speed, Vo is fluid free flow velocity (ocean currents), and S is turbine cross-section area.

Figure 4 shows the relationship betweet TSR with Cp, shown below.

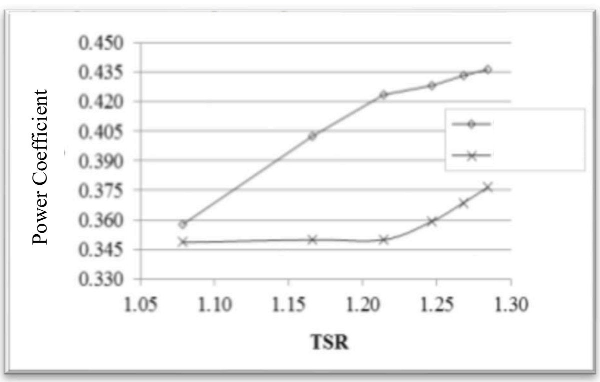

Figure 4. Relationship of TSR with Cp

A form of energy conversion is impossible to have 100 percent efficiency. If that happens, the kinetic energy will be zero. Turbines with a low aspect ratio have a higher power coefficient.

2.5 Hydrodynamic Aspects of Hydrofoil

When placed in a water flow, Geometry will produce a lift that is bigger than drag force. In the law of action-reaction, Issac Newton once stated that if object A exerts a force on object B, object B will also react to object A. This law is the same as the relationship between lift force and drag force on a hydrofoil. The lift force on the helical turbine is located when ocean currents push water toward the helical blade. The lift force will be reduced when pounding the turbine blade. The reduced lift force was due to the existence of the drag force because there was friction between the ocean currents and the turbine blade. Therefore, the shape of the hydrofoil, the angle of attack (pitch), the speed of the current, and the number of blades play an important role in determining the power output from the turbine. Figure 5 bellow show the lift force and drag force.

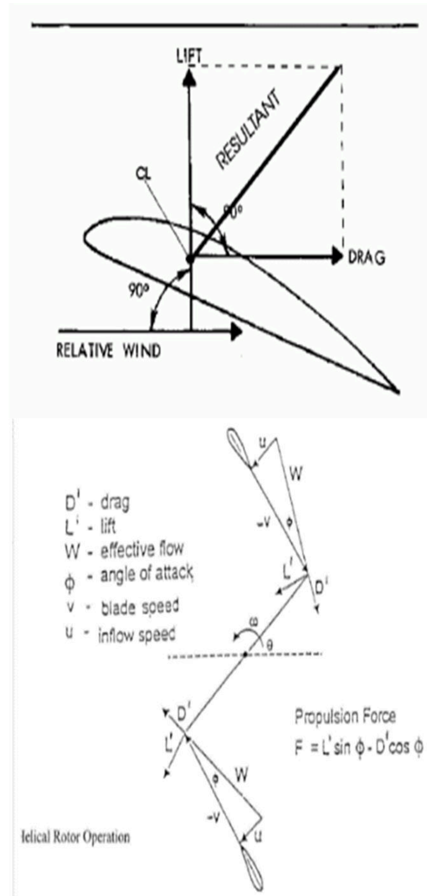

Figure 2.5 Lift force and Drag force

$$Cl = \frac{L}{\frac{1}{2}\rho A V^2} = \frac{2L}{\rho A V^2} \tag{4}$$

$$Cd = \frac{Fd}{\frac{1}{2}\rho A V^2} = \frac{2Fd}{\rho A V^2} \tag{5}$$

Information:

Cl	= lift coefficient
Cd	= drag coefficient
L	= lift style
Fd	= drag style
A	= turbine cross section
V	= free-flow fluid

Here are the pictures and terms in the helical turbine blade show in figure 6 below.

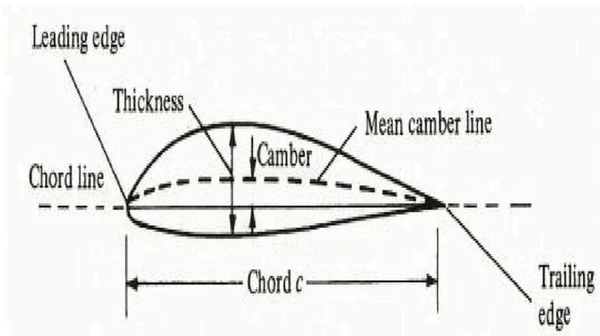

Figure 6. Hydrofoil (Source: http://www.pilotfriend.com/)

Information:
a. Leading Edge is the very front of a hydrofoil
b. Trailing Edge is the very back of a hydrofoil.
c. Chamber line is a line that divides equally between the upper and lower surfaces of the mean chamber line hydrofoil.
d. Chord line is a straight line connecting the leading edge with the trailing edge.
e. Chord (c) is the distance between the leading edge and the trailing edge.
f. Maximum chamber is the maximum distance between the mean camber line and the chord line. The maximum position of the chamber is measured from the leading edge in the form of a chord percentage.
g. Maximum thickness is the maximum distance between the upper and bottom surfaces of the hydrofoil, which is also measured perpendicular to the chord line.

2.6 Computational Fluid Dynamics

CFD or Computational Fluid Dynamics is a method commonly used to analyze the interaction between fluid flows and solid objects. This method emerged around 1970 by combining physical problems, numerical computation, and computer science. In CFD analysis, experiments are carried out based on physical properties such as speed, pressure, temperature, density, and viscosity. The various kinds of physical properties mentioned must be considered simultaneously to produce analytical solutions of physical phenomena related to fluid flow virtually.

In analyzing fluid flow, a mathematical model and a numerical method of a physical case is required, as well as verification to provide accuracy in completing the analysis. The working principle of CFD itself is to perform discretization to solve numerical equations in a smaller set volume. Each adjusting volume is solved iteratively by the regulatory equations, including the law of conservation of mass, momentum, and energy [5]. The help of computer hardware and software is needed to perform discrete calculations to solve problems according to their physical conditions. There are three primary stages in operating the CFD, namely the pre-processor, solver, and post-processor.

a. Pre-processor

At this stage, parameters are input such as the speed of the fluid before passing through the turbine, the speed after exiting the turbine, and the boundary condition must also be defined. The meshing process is also carried out so that the desired results are close to the real results. The more meshes, the more accurate the results.

b. Solver

At this stage, the model of the helical turbine is run with parameters already input during the pre-processing stage. The simulation will stop when the analysis results appear.

c. Post-processor

The final stage, post-processing, is when the results of computational numerical analysis are interpreted into images, graphics, and even animations with specific color patterns.

3. RESEARCH METHODOLOGY

The stages of this research consisted of a literature study, validation, to the analysis and conclusions described below:

1. Literature Study
Authors seek a theoretical basis specifically regarding the helical turbine, ocean current energy and seek references about CFD to support research in this thesis. These references, authors were collected from various local, international journals, books, and the internet.
2. Data Preparation
At this stage, collecting and preparing supporting data is carried out. The data is 3D CAD design in the form of the helical turbine. The specifications of the turbine type are NACA 0012 (secondary data for design validation).
3. CFD simulation
The data prepared has previously been entered into ANSYS Fluent software. In this study, the authors vary the hydrofoil thickness and the inclination angle of blades for the moment coefficient.
4. Interpretation of CFD Simulation Results
CFD simulation results in the form of moment coefficients. The moment coefficient is then formulated to look for torque.
5. Validation
Validation is done to know that the results of the running model are the same as the results in the secondary data. The results of the torque from the author's numerical simulation will be graphed. The graph will be compared with the validation graph from secondary data.
6. Changes in Parameters
Changes in parameters were made to determine differences in the final results. Changes in this study consisted of two variables, namely the hydrofoil thickness (NACA 0010, 0016, 0020) and the inclination angle of blades (25^0 and 60^0).
7. Analysis of Results and Conclusions
At this stage, data analysis was performed and processed in curves, graphs and tables. Conclusions can

be drawn based on the problems and objectives of this thesis research.

4. ANALYSIS OF RESULTS AND DISCUSSION

4.1 Mesh Accuracy Analysis

Several experiments have been carried out from a small mesh, around 800,000 elements to 4,000,000 elements in this study. In the case of very few elements, convergence cannot be achieved and finally, a divergence condition occurs, which means that the number of elements must be increased. Finally, the authors decided to arrange elements with a range of 3,000,000 to 4,000,000 elements. In this model, a single running steady-state simulation takes ± 120 minutes with the ability of a standard computer (CPU Core Duo) with 8 gigabytes of RAM. At the same time, the transient state simulation takes ± 36 hours for 3 turbine rotations.

4.2 Validation

The following is a comparison table between the experimental results, MRF, and Transient methods with TSR 1.4 and 110 RPM.

Table 4. Comparison of experimental torque data and steady state simulation

Numeric vs Experiment			
Azimuthal Angle	Steady mesh (800.000)	Steady mesh (4.000.000)	Experiment
0	0.95	1.3	1.27
30	0.60	1	0.85
60	0.76	1.16	1.2
90	1.00	1.3	1.5
120	0.96	0.81	0.88
150	0.43	0.76	0.7
180	0.95	1.3	1.27
210	0.60	1	0.85
240	0.76	1.16	1.2
270	1.10	1.3	1.5
300	0.98	0.81	0.88
330	0.43	0.76	0.7
360	0.95	1.3	1.27

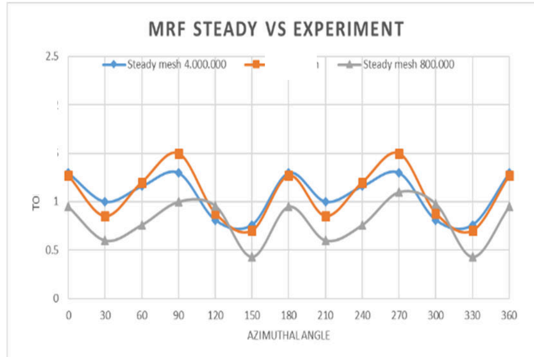

Figure 7. Comparison of Steady MRF and Experimental

The comparison between experimental and transient is as the data below. The authors include the results of running the transient method 6 times, but the comparison is made on the 6th round.

Table 2. Comparison of experimental torque data and transient state simulation

Transient vs Experiment		
Azimuthal Angle	Numeric (Transient)	Experiment
0	0.99	1.27
30	1.70	0.85
60	1.84	1.2
90	1.45	1.5
120	0.94	0.88
150	0.54	0.7
180	0.96	1.27
210	1.70	0.85
240	1.84	1.2
270	1.45	1.5
300	0.94	0.88
330	0.54	0.7
360	0.99	1.27

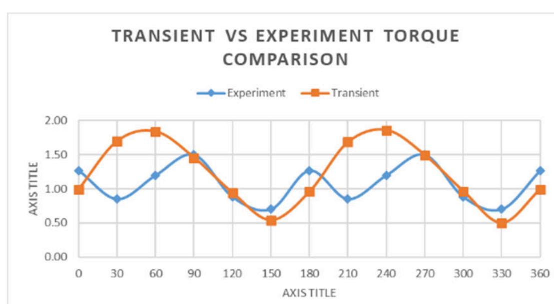

Figure 8. Comparison of Experimental Torque Charts and Transient State Simulation Results

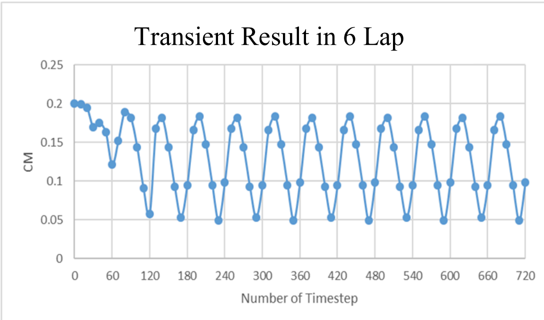

Figure 9. CM graph of NTS

The following is the comparison of the torque values from the results of the steady-state, experimental, and transient state simulation:

Table 3. Experimental torque data, steady-state simulation and transient state simulation

Comparison of Numerical Calculations with Experiments				
Azimuthal Angle	Steady mesh (800.000)	Steady mesh (4.000.000)	Transient mesh (4.000.000)	Experiment
0	0.95	1.30	0.99	1.27
30	0.60	1.00	1.70	0.85
60	0.76	1.16	1.84	1.20
90	1.00	1.30	1.45	1.50
120	0.96	0.81	0.94	0.88
150	0.43	0.76	0.54	0.70
180	0.95	1.30	0.96	1.27
210	0.60	1.00	1.70	0.85
240	0.76	1.16	1.84	1.20
270	1.10	1.30	1.45	1.50
300	0.98	0.81	0.94	0.88
330	0.43	0.76	0.54	0.70
360	0.95	1.30	0.99	1.27

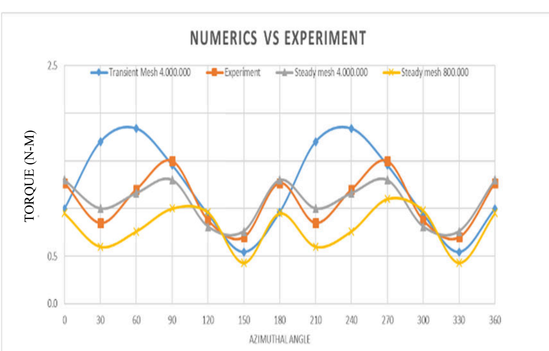

Figure 10. Experimental Data Torque Graph, Steady State Simulation and Transient State

After the authors manage the data above, it is found that the average error of the steady MRF method with mesh is 800,000 and 4,000,000 by 28% and 8%, respectively. Whereas in the Transient method with mesh 4,000,000, the average error was 23%. A large error in the Transient method is because transient simulations require more turns and a larger mesh than the steady method. Therefore, to simulate variations in this thesis, the authors use the MRF steady method with a mesh of 3,000,000 to 4,000,000 with laminar flow patterns.

4.3 Variations in the Hydrofoil Thickness

One of the variations developed in this thesis is Hydrofoil Thickness. The thicker the hydrofoil, the structure that hits the fluid will further increase the torque. On the other hand, the thinner the turbine torque decreases. However, at specific thicknesses, a stall condition may occur. The stall condition occurs due to the vortex shed, which produces turbulence which reduces the lift force. This shows that changes in the variables in hydrofoil thickness can affect the torque generated by the Gorlov turbine.

Table 4. Comparison of Turbine Torque with NACA 0010, 0012, 0016, 0020

Comparison of Torque				
Azimuthal Angle (^{0})	Torque (N-m)			
	NACA 0010	NACA 0012 (Validation)	NACA 0016	NACA 0020
0	1.00	1.3	1.72	1.13
30	1.20	1	1.90	1.21
60	1.22	1.16	2.01	1.27
90	0.95	1.3	1.76	1.15
120	0.50	0.81	1.58	0.98
150	0.47	0.76	1.40	0.85
180	1.00	1.3	1.72	1.13
210	1.20	1	1.90	1.21
240	1.22	1.16	2.01	1.27
270	0.95	1.3	1.76	1.15
300	0.50	0.81	1.58	0.98
330	0.47	0.76	1.40	0.85
360	1.00	1.3	1.72	1.13

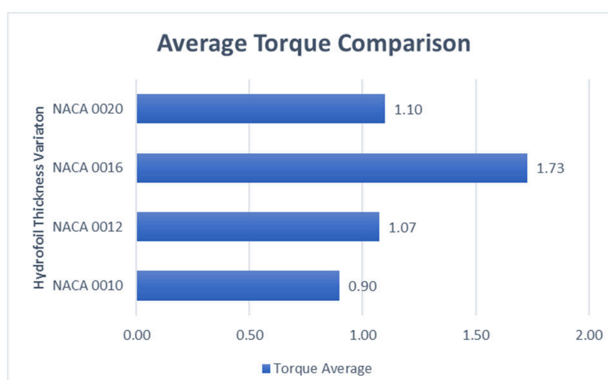

Figure 11. Graph of comparison of turbine torque average

with hydrofoil thickness variations.

From the table and graph above, the torque of the turbine with NACA 0016 is the greatest. It can also be seen that the NACA 0020 has also experienced a decrease in torque or reached a stall condition. The stall condition occurs due to vortex shedding, which reduces the lift force. This shows that changes in the variation in hydrofoil thickness influenced the torque generated by the Gorlov turbine. However, at specific thicknesses a stall condition can occur.

4.3 Variations in the Inclination Angle of Blades

The variation of the inclination angle significantly affects the stability of the torque. In this simulation, the hydrofoil model with NACA 0012 and NACA 0016 is used, with variations of 25^0 and 60^0 inclination angle of blades.

Table 4. Comparison of Turbine Torque with variations of 25^0 and 60^0 inclination angle of blades.

Comparison of of Turbine Torque with variations of 25° and 60° Inclination Angle of Blades				
Azimuthal Angle (°)	Torque (N-m)			
	NACA 0012 Inclination Angle 25°	NACA 0012 Inclination Angle 43.68°	NACA 0012 Inclination Angle 60°	NACA 0016 Inclination Angle 60°
0	0.78	1.3	2.01	2.24
30	0.50	1	2.90	3.13
60	0.60	1.16	2.30	3.15
90	0.78	1.3	1.76	2.45
120	0.84	0.81	0.02	0.64
150	0.77	0.76	0.15	0.32
180	0.78	1.3	2.01	2.24
210	0.50	1	2.90	3.13
240	0.60	1.16	2.30	3.15
270	0.78	1.3	1.76	2.45
300	0.84	0.81	0.02	0.64
330	0.77	0.76	0.15	0.32
360	0.78	1.3	2.01	2.24

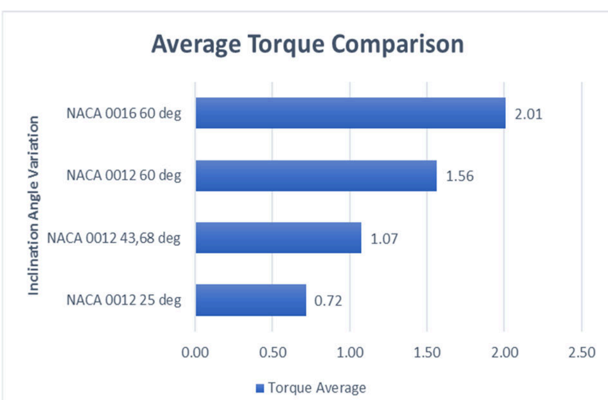

Figure 12. Graph of Comparison of Turbine Torque Average with inclination angle of blades variations.

From the simulation results, it can be seen in the graph above, the smaller the inclination angle of the blades, the less torque generated. This is because the blades in the upstream area block the blades in the downstream area. Then, at the large inclination angle of the blades, there is a large fluctuation of torque. This can happen because water is easily entering the turbine without touching the blades, due to the large inclination angle of the blades.

Here follows a comparison of the turbine efficiency of all the variables if searched by the formula.

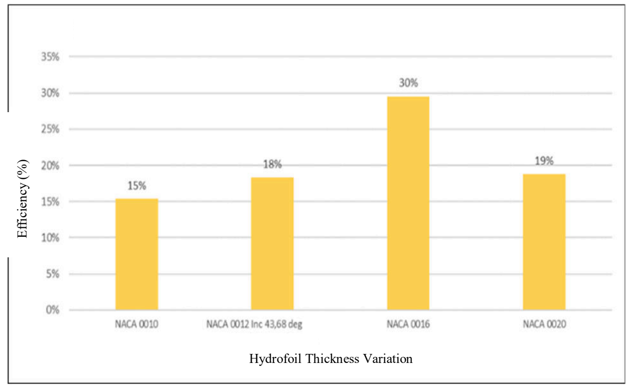

Figure 12. Graph of Comparison of Turbine Efficiency with Hydrofoil Thickness Variations

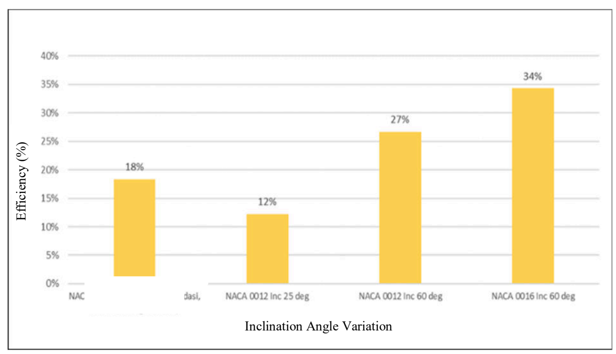

Figure 13. Graph of Comparison of Turbine Efficiency with Inclination Angle of Blades Variations

5. CONCLUSION

Based on the results of numerical simulations, data analysis, and discussions that have been done, several conclusions can give in this paper:

- The thicker the hydrofoil, the more fluid hits the structures and will increase the torque. However, at specific thicknesses, there is a possibility of a stall condition. The stall condition occurs due to vortex shedding, which reduces the lift force. It is recommended to choose a hydrofoil thickness below NACA 0020 which has reached the stall condition.
- Variations in the inclination angle of the blade significantly affect the stability of the resulting torque. The smaller the inclination angle of the blades, the less torque generated. Then, at the large inclination angle of the blades, there is a large fluctuation of torque. This can happen because water is quickly entering the turbine

without touching the blades due to the large inclination angle of the blades.

- The highest efficiency of all variations, hydrofoil thickness and inclination angle of blades is the turbine using NACA 0016 with 60^0 of inclination angle.

REFERENCES

[1] Republik Indonesia, 2017. Peraturan Menteri Energi dan Sumber Daya Mineral Nomor 39 Tahun 2017 tentang Pelaksanaan Kegiatan Fisik Pemanfaatan Energi Baru dan Energi Terbarukan serta Konservasi. Jakarta.

[2] Bappenas. 2014. Ketahanan Energi Indonesia: Gambaran Permasalahan dan Strategi Memperbaikinya. Bappenas. Edisi XX.

[3] Ahmadi-Baloutaki M., 2015. Analysis and Improvement of Aerodynamic Performance of Straight Bladed Vertical Axis Wind Turbines. Electronic Theses and Dissertation Windsor University, Ontario, Canada.

[4] Khan, M.J, Bhuyan, G., Iqbal, M.T., & Quaicoe, J.E. 2009. 'Hydrokinetic energy conversion systems and assessment of horizontal and vertical axis turbines for-river and tidal applications: A technology status review', Applied Energy, vol. 86, issue 10, pp. 1823-1835.

[5] Blazek, J., 2007. Computational Fluid Dynamics Principles and Applications. Oxford: Butterworth-Heinemann.

[6] Kasharjanto, et al. 2017. Study of the Utilization of Sea Current Energy in Indonesia. Wave Journal. Volume 11: 2.

[7] Rivantoro, F and Irfan, S. A. 2015 Study of Selection of Design of Sea Current Power Plant (PLTAL) Using Analytical Hierarchy Process (AHP) Method. ITS Engineering Journal. Volume 4: 2.

[8] Pongduang, S., Kayankannavee, C., Tiaple, Y., 2015. 'Experimental Investigation of Helical Tidal Turbine Characteristics with Different Twists', International Conference on Alternative Energy in Developing Countries and Emerging Economies, vol. 79. pp. 409 – 414.

[9] Hestyandhoko. 2009. Optimization of Blade Design in Horizontal Axle Wind Turbines to Meet the Squid Fishing Vessel Lighting Power Needs. Thesis. Department of Shipping Engineering FTK ITS: Surabaya.

[10] Satrio D, Suntoyo and Ramadhan L I 2022 The advantage of flow disturbance for vertical-axis turbine in low current velocity Sustain. Energy Technol. Assessments 49 101692 1-9

[11] Dendy Satrio, Andreas Anthoni Wiyanto, Mukhtasor. 2022. IN-SITU EXPERIMENT OF CROSS-FLOW SAVONIUS HYDROKINETIC TURBINE WITH A DEFLECTOR. Journal of Marine-Earth Science and Technology. Vol 3. Pp 1-4.

[12] Elyas Nur Fridayana, Yoyok Setyo Hadiwidodo, Dendy Satrio, Elysa Nensy Irawan. 2022. Studi Model Turbulensi pada Vertical Axis Water Turbine (VAWT) Menggunakan Metode Computational Fluid Dynamics (CFD). Syntax Literate; Jurnal Ilmiah Indonesia. Vol. 7. Pp 8844-8863.

[13] Satrio D, Firdaus Yusri M, Mukhtasor, Rahmawati S, Junianto S and Musabikha S 2022 Numerical simulation of cross-flow Savonius turbine for locations with low current velocity in Indonesia J. Brazilian Soc. Mech. Sci. Eng. 44 1–11